(Revised)

Mesoporous silicas containing carboxylic acid: Preparation, thermal degradation, and catalytic performance

Sadanobu Sumiya[a,b], Yuka Kubota[a], Yasunori Oumi[a], Masahiro Sadakane[a], Tsuneji Sano[a,*]

[a] Department of Applied Chemistry, Graduate School of Engineering, Hiroshima University, Higashi-Hiroshima 739-8527, Japan

[b] Taki Chemical Co., Ltd., 2 Midorimachi, Befu-cho, Kakogawa-shi, Hyogo 675-0124, Japan

*Corresponding author. Fax: +81-82-424-5494; Tel: +81-82-424-7607; E-mail: tsano@hiroshima-u.ac.jp

Abstract

The calcination and thermal degradation behaviors of surfactants in mesoporous silicas SBA-15 and MCM-41 were investigated by FT-IR, ^{13}C CP/MAS NMR, TG/DTA, and GPC. It was found that carboxylic acid–containing products were generated as active

components in the mesopores of SBA-15 and MCM-41 from the triblock copolymer $(PEO)_{20}(PPO)_{70}(PEO)_{20}$ and cetyltrimethylammonium bromide (CTAB), respectively; the latter materials were used as templates. The carboxylic acid–containing mesoporous silica obtained showed a catalytic activity for hydrolysis of sucrose. The acidity was evaluated by means of NaOH titration. The acidity sensitively depended on both the calcination temperature and the atmosphere; the maximum appeared at 150 °C in air for SBA-15 where the highest activity was observed. However, the product in MCM-41 showed a lower catalytic activity than that in SBA-15. The SBA-15 product was easily leached from the mesopores of SBA-15 into the solution, but the degree of leaching for MCM-41 was considerably smaller than that for SBA-15.

Keywords

Carboxylic acid, Degradation, Surfactant, SBA-15, MCM-41, Sucrose hydrolysis

1. Introduction

Considerable attention has been focused on the catalytic applications of mesoporous materials such as MCM-41 and SBA-15, which exhibit high surface areas and well-ordered pore systems with pore diameters in the range 1.5–30 nm [1–10]. Purely

siliceous mesoporous materials have chemically inert frameworks; consequently, they lack acid sites. Therefore, many studies have investigated the incorporation of various metals such as Al, Ga, Ti, and V into the frameworks of mesoporous silicas [11–21]. However, the acidities of these metal-incorporated mesoporous silicas are much weaker than that of zeolite.

Recently, with a view to expanding the scope of catalytic applications of mesoporous materials, several studies have reported the synthesis of mesoporous silicas functionalized with sulfonic [22–28] and carboxyl groups [29, 30]. These functionalized mesoporous materials can be synthesized by the oxidation of mesoporous silicas containing thiol (-SH) and cyano (-CN) groups; these silicas are prepared either by silylation with mercaptopropyl trimethoxysilane (MPTMS) and cyanoethyltriethoxysilane (CETES) or by a one-step hydrolysis and co-condensation of alkoxysilanes and MPTMS or CETES. However, these synthesis methods are inconvenient because they involve multiple-steps; in fact, it has been observed that the use of a strong oxidant such as H_2O_2 leads to the destruction of a part of the mesoporous silica framework [31].

The synthesis of mesoporous silica involves the use of surfactant micelles as templates for the assembly and subsequent condensation of silica sources, followed by

the removal of the surfactants. The surfactants are usually removed by calcination at high temperatures. Although the influence of calcination on the physicochemical properties of mesoporous silica has been widely investigated [32–37], few studies have reported the calcination and thermal degradation behavior of the surfactant in the mesopores [37,38]. After conducting detailed analyses such as ^{13}C MAS NMR, FT-IR, and mass spectrometry, Kaliaguine et al. reported that terminal formate groups (O=CH-O-) were generated during the thermal degradation of a surfactant triblock copolymer in the mesopores of SBA-15 [38].

In this study, we investigated the calcination and thermal degradation behaviors of surfactants, triblock copolymer and cetyltrimethylammonium bromide, used as templates in mesoporous silicas SBA-15 and MCM-41, respectively, and we proposed a simple method for the preparation of carboxylic acid–containing products in the mesopores by the calcination and thermal degradation of a surfactant. The catalytic performance of the acid produced in the mesopores was evaluated by measuring the sucrose hydrolysis reaction, which is considered to be a model reaction for hydrolysis of a polysaccharide such as starch or cellulose by using solid acid catalysts.

2. Experimental

2.1. Materials

SBA-15 and MCM-41 mesoporous materials were prepared according to the literatures [7,39], with amphiphilc triblock copolymer poly(ethylene oxide)$_{20}$-poly(propylene oxide)$_{70}$-poly(ethylene oxide)$_{20}$ ($PEO_{20}PPO_{70}PEO_{20}$, average molecular weight 5800, Aldrich) and cetyltrimethylammonium bromide (CTAB) being used as the templates for SBA-15 and MCM-41, respectively. The solid products were separated by filtration, washed with deionized water, and then dried at 70 °C for 12 h. The calcination and thermal degradation of the surfactants in as-synthesized SBA-15 and MCM-41 were carried out in air or N_2 (200 ml min^{-1}) at various temperatures ranging from 120 to 550 °C for 8 h; the heating rate in the thermal treatments was fixed at 0.9 °C min^{-1}.

2.2. Characterization

X-ray diffraction (XRD) patterns were collected using a powder X-ray diffractometer (Bruker, D8 Advance) with graphite monochromatized Cu Kα radiation at 40 kV and a tube current of 40 mA. Nitrogen adsorption-desorption isotherms at –196 °C were measured using a conventional volumetric apparatus (Bel Japan, BELSORP Mini). Prior to the adsorption measurements, the samples (ca. 0.1 g) were heated at 100 °C for 10 h

in a nitrogen flow. The surface areas were calculated by the Brunauer-Emmet-Teller (BET) method and the pore diameters by the Barrett-Joyner-Halenda (BJH) method. Thermal analysis was carried out using a thermal gravimetry–differential thermal analysis (TG/DTA) apparatus (SSC/5200 Seiko Instruments). A sample of ca. 3 mg was heated in a flow of air (50 ml min^{-1}) at 5 °C min^{-1} from room temperature to 800 °C. ^{13}C CP/MAS NMR spectra were recorded using a 7-mm-diameter zirconia rotor on a Bruker Avance DRX-400 at 100.6 MHz. The rotor was spun at 6 kHz. The spectra were accumulated with 6.0-μs pulses, a 25 s recycle delay, and 1000 scans. Glycine (H_2NCH_2COOH) was used as a chemical shift reference. Infrared (IR) spectra were recorded on a Fourier transform infrared (FT-IR) spectrometer (JEOL JIR-7000) with a resolution of 4 cm^{-1} at room temperature. Each sample was pressed into a self-supporting thin wafer (ca. 10 mg cm^{-2}) and placed into a quartz IR cell equipped with CaF_2 windows. Prior to measurements, each sample was dehydrated under vacuum at room temperature for 0.5 h. For acidity measurement, pyridine adsorption was also carried out at room temperature for 1 h, followed by degassing at room temperature for 0.5 h. The average molecular weights of the carboxylic acid–containing products removed from the mesoporous materials were measured by gel permeation chromatography (GPC) using a Waters 150 CV system at room temperature with

tetrahydrofuran as a solvent.

2.3. Hydrolysis of sucrose

The batch-mode hydrolysis of sucrose was performed in a glass reactor. In general, 0.2 g of sucrose was dissolved in 10 ml of H_2O, and 0.1 g of catalyst was then added to the solution. The resulting mixture was stirred at 80 °C for 4 h. The products were analyzed by liquid chromatography (Shimadzu LC-2010C, Column Shodex SUGAR SH1011, I.D. 8 mm × L300 mm) with a refractive index detector. Five mmol l^{-1} $HClO_4$ was used as an eluent.

3. Results and discussion

3.1. SBA-15

Figure 1 shows the XRD patterns of SBA-15 samples calcined at various temperatures in air and in N_2. For the SBA-15 samples calcined at >120 °C in air and at >300 °C in N_2, a well-resolved pattern with a strong peak (100) and two weak peaks (110) and (200) was observed at around 2 theta = 1–2°, which is characteristic of SBA-15 [7]. Some of the physicochemical properties are summarized in Table 1. The surface area and pore volume increased with the calcination temperature, reaching

maximum values at 300 °C in air and at 400 °C in N_2, and the values gradually decreased as the calcination temperature was increased further. This reduction can be attributed to lattice shrinkage by condensation of the silanol groups [37]. At various calcination temperatures, the organic contents of the SBA-15 samples calcined in air were smaller than those in N_2, indicating that calcination in air led to decomposition of the triblock copolymer at a relatively low temperature as compared to calcination under an inert atmosphere.

To acquire information about the organics produced from the triblock copolymer in the mesopores, we characterized the obtained SBA-15 samples by ^{13}C CP/MAS NMR and FT-IR. Several peaks were observed in the ^{13}C CP/MAS NMR spectrum of as-synthesized SBA-15 [Fig. 2(A), (B)-(a)]. Methine carbons, methylene carbons, and methyl carbons of the propylene oxide (PO) units were observed at 75.9, 73.9, and 18.3 ppm, respectively, while methylene carbons of the ethylene oxide (EO) units were observed at 71.3 ppm [40]. For calcination in air, the intensities of these peaks decreased with an increase in the calcination temperature and disappeared completely after calcination at 300 °C [Fig. 2(A)-(d)]. In the spectra of the SBA-15 samples calcined at 120 °C and 150 °C in air, a new peak assigned to the carboxyl groups [-(C=O)O-H] was observed at ca. 165 ppm [Fig. 2(A)-(b) and (c)]. This peak also

disappeared after calcination at 300 °C. However, in the case of calcination in N_2, the peak at ca. 165 ppm was not observed and the peaks of the PO and PE units were visible even after calcination at 300 °C [Fig. 2(B) - (c)].

Figure 3 shows the FT-IR spectra of the SBA-15 samples calcined in air and in N_2. Peaks assigned to the bending vibration of the C-H groups of the triblock copolymer were observed between 1300 and 1500 cm^{-1}. The intensities of these peaks gradually decreased with an increase in the calcination temperature. In the case of calcination in air, these peaks almost disappeared after calcination at 200 °C. On the other hand, in the case of calcination in N_2, these peaks were still observed even after calcination at 300 °C. In addition, for the SBA-15 samples calcined at 120–200 °C in air, a new peak assigned to the carbonyl groups (C=O) was observed at ca. 1730 cm^{-1}. The SBA-15 calcined at 150 °C exhibited the highest peak intensity. Although calcination in N_2 at 200 and 300 °C also yielded the peak at ca. 1730 cm^{-1}, the peak intensity was considerably weaker. These results strongly indicate the generation of carboxyl groups in the mesopores of SBA-15.

To confirm this hypothesis, we carried out sucrose hydrolysis, which requires Brönsted acidic sites [41], on the SBA-15 samples. Figure 4 shows the sucrose conversion results for the SBA-15 samples calcined at various temperatures in air and in

N_2. For calcination in air, the sucrose conversion value strongly depended on the calcination temperature. SBA-15 calcined at 150 °C in air exhibited the highest conversion. On the other hand, for calcination in N_2, the sucrose conversion value was almost constant (ca. 8%). The tendency of sucrose conversion to depend on the calcination temperature was closely correlated to the behaviors governing the peak intensities at ca. 165 ppm in the ^{13}C CP/MAS NMR spectra (Fig. 2) and at ca. 1730 cm^{-1} in the IR spectra (Fig. 3). Therefore, we conclude that products containing carboxylic acid [-(C=O)O-H] are generated in the mesopores of SBA-15 by the calcination and thermal decomposition of the triblock copolymer.

The presence of acidic protons in the products was evaluated by pyridine adsorption. In the IR spectrum shown in Fig. 5, several peaks attributable to pyridinium ion on Brönsted acid sites (1538 and 1640 cm^{-1}) and hydrogen-bonded pyridine (1444 and 1595 cm^{-1}) were observed. Two peaks at 1577 and 1623 cm^{-1} can be assigned to physically adsorbed pyridine. This indicates strongly the presence of surface acidic protons. To evaluate the acidity of the carboxylic acid–containing products in the mesopores, therefore, the amounts of acid were measured by titration with a 5 mmol l^{-1} NaOH solution. Figure 6 shows the relationship of the amount of acid in SBA-15 calcined in air and in N_2 with the calcination temperature. For calcination in air, the

amount of acid reached a maximum value at 120 °C and decreased with the calcination temperature. On the other hand, for calcination in N_2, the amount of acid was considerably smaller. This indicates the formation of a large number of carboxyl groups in the mesopores of SBA-15 calcined in air. Figure 7 shows the turnover number (TON) for sucrose hydrolysis over SBA-15 samples calcined at various temperatures in air. The TON was defined as moles of sucrose converted (moles of acid amount)$^{-1}$. The TON clearly depended on the calcination temperature, with the highest TON (ca. 30) at 300 °C, indicating that the acidity of the product depended on the calcination temperature. These results indicate that the reaction catalytically proceeds.

Next, to clarify the possibility of leaching the carboxyl acid–containing product from the mesopores, we subjected SBA-15 previously calcined at 150 °C in air to repeated runs of hydrolysis. The first run of SBA-15 gave a sucrose conversion of 68%. The used catalyst was subsequently collected by filtration, washed with deionized water, and then reused in the second reaction run. This procedure was repeated three times. The sucrose conversion was 3% for the second run and 0% for the third run. To elucidate these differences in the sucrose conversion, we measured the IR spectra of the SBA-15 samples before and after sucrose hydrolysis. Figure 8 shows peaks at ca. 1730 cm^{-1} and 1300–1500 cm^{-1}, which are respectively assigned to the carboxyl groups and to the C-H

groups that disappeared after the reaction; this result indicates that the catalyst component with the carboxyl groups leached into the reaction mixture. To further confirm this, we carried out the following experiments. SBA-15 calcined at 150 °C in air was dispersed in deionized water and stirred at 80 °C for 4 h. Then, the mixture was filtered and the filtrate was analyzed. The sucrose conversion for the filtrate was similar to that for SBA-15 calcined at 150 °C in air, indicating that the active component generated by the calcination and thermal degradation of the triblock copolymer was easily leached from the SBA-15 mesopores into the solution.

The average molecular weight of the active component leached from the mesopores was evaluated by GPC. The GPC curve showed only one peak. The average molecular weight was calculated to be ca. 1100. This suggests that the triblock copolymer $(PEO)_{20}(PPO)_{70}(PEO)_{20}$ (average molecular weight: 5800) was decomposed to form fragments with an average molecular weight of ca. 1100 during calcination at 150 °C in air. Although the exact chemical structure of active component and the formation mechanism are not clarified at the present stage, we speculate that the active component has terminal carboxyl groups at both ends.

3.2. MCM-41

MCM-41 was synthesized using a cationic surfactant, CTAB ($C_{16}H_{33}(CH_3)_3N^+Br^-$), as a template. The mesopore size of MCM-41 is smaller than that of SBA-15. To elucidate the influence of the mesopore size and the chemical composition of the surfactant, we investigated the calcination and thermal degradation behavior of CTAB in the mesopores of MCM-41, along with its catalytic activity. Based on the above results for SBA-15, the calcination and the thermal degradation of CTAB were carried out only in air.

Table 2 summarizes the various characteristics of MCM-41 samples calcined at various temperatures, such as the surface area, pore volume, and organic content. In comparison with the case of SBA-15, the oxidation and decomposition of the organic template in MCM-41 clearly began at a relatively higher temperature, probably due to differences in mesopore size and chemical composition between SBA-15 and MCM-41. Figure 9 shows the IR spectra of MCM-41 samples calcined at various temperatures. For as-synthesized MCM-41, peaks assigned to the bending vibration of the C-H groups of CTAB were observed between 1300 and 1500 cm^{-1}. On the other hand, for MCM-41 samples calcined at 200–350 °C, peaks assigned to the C=O and C=C groups were observed at ca. 1730 and ca. 1630 cm^{-1}, respectively. A peak was also observed at ca. 1780 cm^{-1}; however, at present, the origin of this peak is unknown. These peaks

disappeared completely after calcination at 400 °C. The observation of the peak at ca. 1730 cm^{-1} strongly indicates the formation of carboxylic acid from CTAB during the calcination process. To confirm the formation of carboxylic acid–containing products in MCM-41, we conducted sucrose hydrolysis on MCM-41 samples calcined at various temperatures. As in the case of SBA-15, the sucrose conversion strongly depended on the calcination temperature (Fig. 10). MCM-41 calcined at 300 °C exhibited the highest conversion. The tendency of the sucrose conversion to depend on the calcination temperature was in good correlation with the behavior underlying the peak intensity at ca. 1730 cm^{-1} in the IR spectra (Fig. 9), suggesting the formation of carboxylic acid–containing products. This was also confirmed from the following facts. The sucrose conversion of MCM-41 calcined at 300 °C in N_2 (ca. 4%) was considerably lower than that of MCM-41 calcined in air (ca. 50%). In the IR spectrum of MCM-41 calcined at 300 °C in N_2, the peak at ca. 1730 cm^{-1} was barely visible (not shown). Table 3 summarizes the amounts of acid in MCM-41 samples calcined in air. The TONs calculated using the acid amounts are also listed. Although the TON values exceeded 1, there was a considerable difference in the TON values between MCM-41 and SBA-15 (Fig. 7). The lower TON value is probably due to the smaller mesopore size.

Finally, to investigate the possibility of product leaching, MCM-41 calcined at

300 °C in air was subjected to repeated runs of hydrolysis; the results are shown in Fig. 11. The experimental procedure was the same as that used for SBA-15. The first run with MCM-41 gave a sucrose conversion of ca. 50%. The sucrose conversion gradually decreased in subsequent runs. Compared to SBA-15, however, the sucrose conversion did not become zero, even after 3 cycles. Figure 12 shows the IR spectra of MCM-41 samples calcined at 300 °C before the reaction and after 3 cycles. Although the peak assigned to the carboxyl groups was clearly observed at ca. 1730 cm^{-1} for both samples, there was a large difference in the peak intensity, indicating the leaching of an active component into the solution. However, the degree of leaching was considerably smaller than for the SBA-15 (Fig. 8).

4. Conclusions

Carboxylic acid–containing products were generated in the mesopores of SBA-15 and MCM-41 during the thermal degradation of the triblock copolymer and CTAB, respectively, which were used as templates. The acidity sensitively depended on both the calcination temperature and the atmosphere. The carboxylic acid–containing products formed from the triblock copolymer were easily leached from the mesopores of SBA-15 into the solution. However, the degree of leaching for MCM-41 was

considerably smaller than that for SBA-15. Thus, our results indicate that functionalized mesoporous materials prepared by surfactant degradation in the mesopores have high potential applicability in catalyst systems.

References

[1] T. Yanagisawa, T. Shimizu, K. Kuroda, C. Kato, Bull. Chem. Soc. Jpn. 63 (1990) 988-992.

[2] S. Inagaki, Y. Fukushima, K. Kuroda, Chem. Commun. (1993) 680-681.

[3] S. Inagaki, A. Koiwai, N. Suzuki, Y. Fukushima, K. Kuroda, Bull. Chem. Soc. Jpn. 69 (1996) 1449-1457.

[4] C.T. Kresge, M.E. Leonowicz, W.J. Roth, J.C. Vartuli, J.S. Beck, Nature 359 (1992) 710-712.

[5] J.S. Beck, J.C. Vartuli, W.J. Roth, M.E. Leonowicz, C.T. Kresge, K.D. Schmitt, C.T.W. Chu, D.H. Olson, E.W. Sheppard, S.B. McCullen, J.B. Higgins, J.L. Schlenker, J. Am. Chem. Soc. 114 (1992) 10834-10843.

[6] Q. Huo, R. Leon, P.M. Petroff, G.D. Stucky, Science 268 (1995) 1324-1327.

[7] D. Zhao, J. Feng, Q. Huo, N. Melosh, G. Fredrickson, B.F. Chmelka, G.D. Stucky, Science 279 (1998) 548-552.

[8] S.A. Bagshaw, E. Prouzet, T.J. Pinnavaia, Science 269 (1995) 1242-1244.

[9] P.T. Tanev, M. Chibwe, T.J. Pinnavaia, Nature 368 (1994) 321-323.

[10] R. Ryoo, J.M. Kim, C.H. Ko, C.H. Shin, J. Phys. Chem. 100 (1996) 17718-17721.

[11] A. Tuel, S. Gontier, R. Teissier, Chem. Commun. (1996) 651-652.

[12] D.Z.R. Tian, W. Tong, J.Y. Wang, N.G. Duan, V.V. Krishman, S.L. Suib, Science 276 (1997) 926-930.

[13] Q. Zhang, Y. Wang, Y. Ohishi, T. Shishido, K. Takehira, J. Catal. 202 (2001) 308-318.

[14] Z. Zhang, J. Suo, X. Zhang, S. Li, Appl. Catal. A: Gen. 179 (1999) 11-19.

[15] A. Sakthivel, S.E. Dapurkar, N.M. Gupta, S.K. Kulshreshtha, P. Selvam, Micropor. Mesopor. Mater. 65 (2003) 177-187.

[16] R. Mokaya, W. Jones, Z. Luan, M.D. Alba, J. Klinowski, Catal. Lett. 37 (1996) 113-120.

[17] S. Sumiya, Y. Oumi, T. Uozumi, T. Sano, J. Mater. Chem. 11 (2001) 1111-1115.

[18] W.H. Zhang, J. Lu, B. Han, M. Li, J. Xiu, P. Ying, C. Li, Chem. Mater. 14 (2002) 3413-3421.

[19] Z. Luan, J.Y. Bae, L. Kevan, Chem. Mater. 12 (2000) 3202-3207.

[20] Z.E. Berrichi, L. Cherif, O. Orsen, J. Fraissard, J.-P. Tessonnier, E. Vanhaecke, B.

Louis, M.J. Ledoux, C.P. Huu, Appl. Catal. A: Gen. 298 (2006) 194-202.

[21] C. Galacho, M.M.L.R. Carrott, P.J.M. Carrott, Micropor. Mesopor. Mater. 100 (2007) 312-321.

[22] J.A. Melero, R.V. Grieken, G. Morales, Chem. Rev. 106 (2006) 3790-3812.

[23] I. Diaz, C.M. Alvarez, F. Mohino, J.P. Pariente, E. Sastre, J. Catal. 193 (2000) 283-294.

[24] D. Das, J.F. Lee, S. Cheng, Chem. Comm. (2001) 2178-2179.

[25] Q. Yang, M.P. Kapoor, S. Inagaki, J. Am. Chem. Soc. 124 (2002) 9694-9695.

[26] F.Y. Yeoh, A. Matsumoto, T. Baba, J. Porous Mater. 16 (2009) 283-289.

[27] K. Nakajima, I. Tomita, M. Hara, S. Hayashi, K. Domen, J.N. Kondo, Adv. Mater. 17 (2005) 1839-1842.

[28] D. Margolese, J.A. Melero, S.C. Chistiansen, B.F. Chmelka, G.D. Stucky, Chem. Mater. 12 (2000) 2448-2459.

[29] C.M. Yang, B. Zibrowius, F. Schuth, Chem. Comm. (2003) 1772-1773.

[30] S. Shen, P.S. Chow, S. Kim, K. Zhu, R.B.H. Tan, J. Colloid. Interface Sci. 321 (2009) 365-372.

[31] I. Diaz, F. Mohino, J.P. Pariente, E. Sastre, Appl. Catal. A: Gen. 205 (2001) 19-30.

[32] C.Y. Chen, H.X. Li, M.E. Davis, Micropor. Mater. 2 (1993) 27-34.

[33] Q. Huo, D.I. Margolese, U. Ciesla, D.G. Demuth, P. Feng, T.E. Gier, P. Sieger, A. Firouzi, B.F. Chmelka, F. Schuth, G.D. Stucky, Chem. Mater. 6 (1994) 1176-1191.

[34] A. Corma, Q. Kan, M.T. Navarro, J.P. Pariente, F. Rey, Chem. Mater. 9 (1997) 2123-2126.

[35] C.Y. Chen, H.X. Li, M.E. Davis, Micropor. Mesopor. Mater. 2 (1993) 17-26.

[36] F. Klietz, W. Schmidt, F. Schuth, Micropor. Mesopor. Mater. 44-45 (2001) 95-109.

[37] F. Klietz, W. Schmidt, F. Schuth, Micropor. Mesopor. Mater. 65 (2003) 1-29.

[38] F. Berube, S. Kaliaguine, Micropor. Mesopor. Mater. 115 (2008) 469-479.

[39] J.M. Kim, J.H. Kwak, S. Jun, R. Ryoo, J. Phys. Chem. 99 (1995) 16742-16747.

[40] C.M. Yang, B. Zibrowius, W. Schmidt, F. Schuth, Chem. Mater. 16 (2004) 2918-2925.

[41] B. H. Hagerdal, K. Skoog, B. Mattiasson, Eur. J. Microbiol. Biotechnol. 17 (1983) 344-348.

Table 1

Characteristics of SBA-15 samples calcined at various temperatures in air and in N_2

Calcination atmosphere	Calcination temperature (°C)	Surface area[a] (m^2g^{-1})	Pore diameter[b] (nm)	Pore volume[b] (cm^3g^{-1})	Content of organic[c] (wt%)
(as-made)	-	-	-	-	58.1
Air	100	9	3.29	0.02	57.6
air	120	812	8.04	0.82	17.3
air	150	858	8.04	0.86	12.9
air	200	864	8.04	0.89	8.5
air	300	977	8.04	0.91	4.3
air	400	856	8.04	0.80	3.1
air	550	752	8.04	0.82	0
N_2	150	17	3.29	0.04	55.3
N_2	200	19	3.29	0.04	50.8
N_2	300	614	8.04	0.76	27.4
N_2	400	950	8.04	1.12	4.5
N_2	550	874	8.04	0.82	4.8

[a]Determined by the BET method.

[b]Determined by the BJH method.

[c]Determined by TG/DTA analysis.

Table 2
Characteristics of MCM-41 samples calcined at various temperatures in air

Calcination temperature (°C)	Surface area[a] (m^2g^{-1})	Pore diameter[b] (nm)	Pore volume[b] (cm^3g^{-1})	Content of organic[c] (wt%)
(as-made)	-	-	-	43.2
150	29	2.00	0.06	38.3
200	587	2.23	0.49	24.6
250	749	2.64	0.66	13.6
300	843	2.79	0.77	11.5
350	886	2.79	0.80	6.5
400	940	2.97	0.87	1.9
500	970	2.97	0.83	0.2

[a]Determined by the BET method.

[b]Determined by the BJH method.

[c]Determined by TG/DTA analysis.

Table 3

Amounts of acid for MCM-41 samples calcined at various temperatures in air and TONs for sucrose hydrolysis

Calcination temperature (°C)	Acid amount[a] (mmol g^{-1})	TON[b]
150	0	0
200	0.06	3.6
250	0.56	4.0
300	0.47	6.4
350	0.37	6.4
400	0.20	7.6
450	0.15	4.8
500	0	0

[a]Amount of acid was determined by titration with 5 mmol l^{-1} NaOH.

[b]TON = Moles of sucrose converted (moles of acid amount) $^{-1}$.

Figure captions

Fig. 1. XRD patterns of SBA-15 samples calcined at various temperatures (A) in air and (B) in N_2: (a) as-synthesized, (b) 120 °C, (c) 150 °C, (d) 200 °C, (e) 300 °C, (f) 400 °C, and (g) 550 °C.

Fig. 2. ^{13}C CP/MAS NMR spectra of SBA-15 samples calcined at various temperatures (A) in air and (B) in N_2: (a) as-synthesized, (b) 120 °C, (c) 150 °C, (d) 300 °C, and (e) 400 °C.

Fig. 3. IR spectra of SBA-15 samples calcined at various temperatures (A) in air and (B) in N_2: (a) as-synthesized, (b) 120 °C, (c) 150 °C, (d) 200 °C, (e) 300 °C, and (f) 400 °C.

Fig. 4. Conversion of sucrose on SBA-15 samples calcined at various temperatures in air (●) and in N_2 (○).

Fig. 5. IR spectrum of pyridine adsorbed on SBA-15 sample calcined at 150 °C in air. B denotes pyridinium ion on Brönsted acid sites and H denotes hydrogen–bonded

pyridine.

Fig. 6. Relationships between the amount of acid and the calcination temperature for SBA-15 calcined in air (●) and in N_2 (○).

Fig. 7. Relationship between TON and calcination temperature for SBA-15 calcined in air.

Fig. 8. IR spectra of SBA-15 samples calcined at 150 °C in air (a) before and (b) after sucrose hydrolysis.

Fig. 9. IR spectra of MCM-41 samples calcined at various temperatures in air: (a) as-synthesized, (b) 150 °C, (c) 200 °C, (d) 250 °C, (e) 300 °C, (f) 350 °C, and (g) 400 °C.

Fig. 10. Conversion of sucrose on MCM-41 samples calcined at various temperatures in air.

Fig. 11. Reusability of MCM-41 samples calcined at 300 °C in air for sucrose hydrolysis.

Fig. 12. IR spectra of MCM-41 samples calcined at 300 °C in air (a) before and (b) after sucrose hydrolysis (3 cycles).

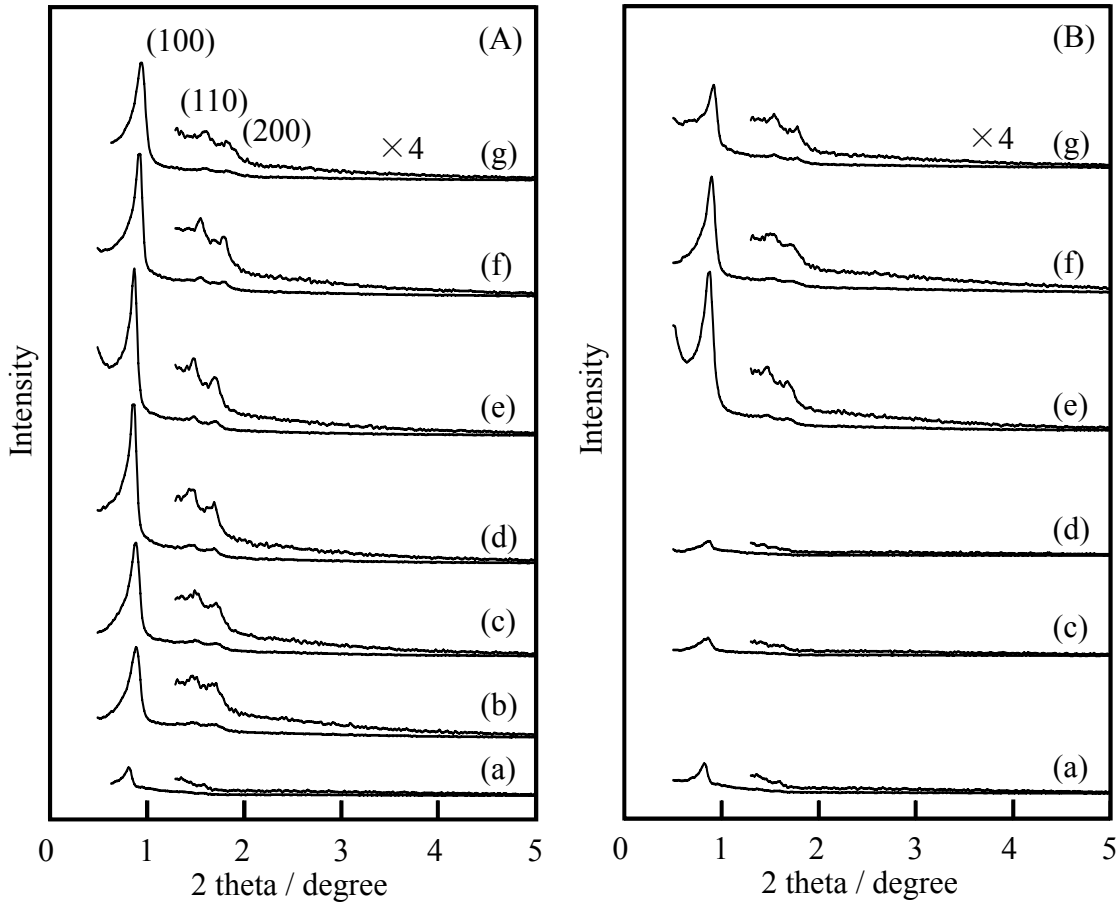
(A)
(100)
(110)
(200)
×4
(g)
(f)
(e)
(d)
(c)
(b)
(a)
Intensity
0
1
2
3
4
5
2 theta / degree
(B)
×4
(g)
(f)
(e)
(d)
(c)
(a)
Intensity
0
1
2
3
4
5
2 theta / degree

Fig. 1

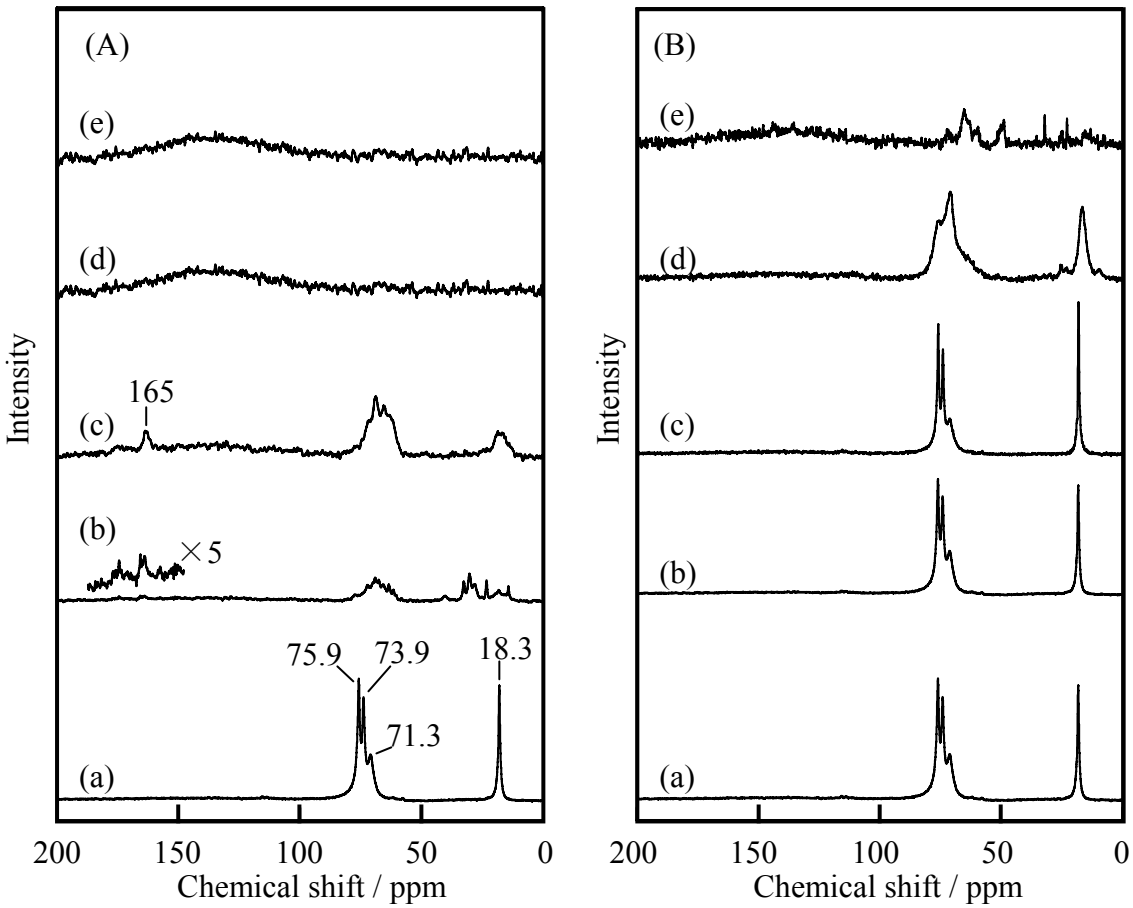
(A)
(e)
(d)
(c)
165
(b)
×5
75.9
73.9
18.3
71.3
(a)
Intensity
200
150
100
50
0
Chemical shift / ppm
(B)
(e)
(d)
(c)
(b)
(a)
Intensity
200
150
100
50
0
Chemical shift / ppm

Fig. 2

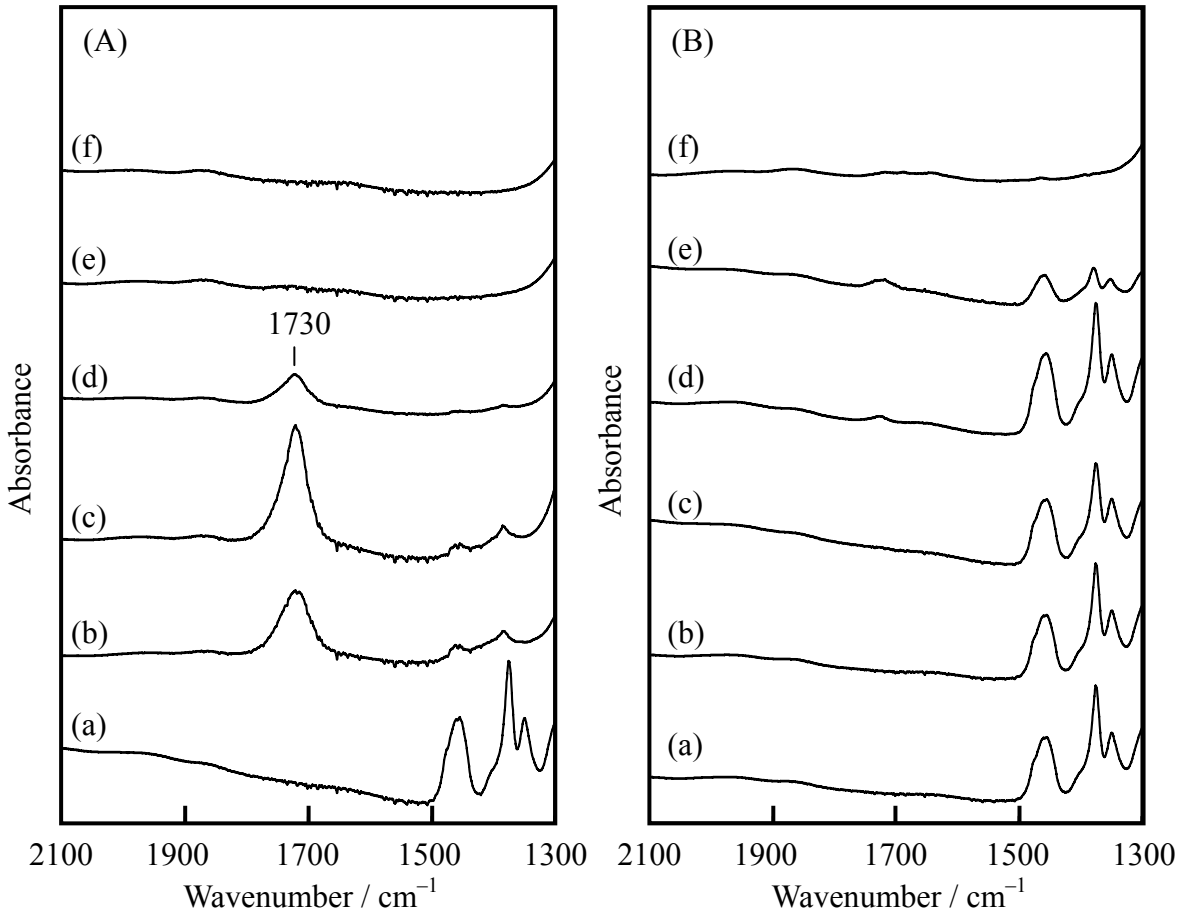
(A)
(f)
(e)
1730
(d)
(c)
(b)
(a)
Absorbance
2100
1900
1700
1500
1300
Wavenumber / cm−1
(B)
(f)
(e)
(d)
(c)
(b)
(a)
Absorbance
2100
1900
1700
1500
1300
Wavenumber / cm−1

Fig. 3

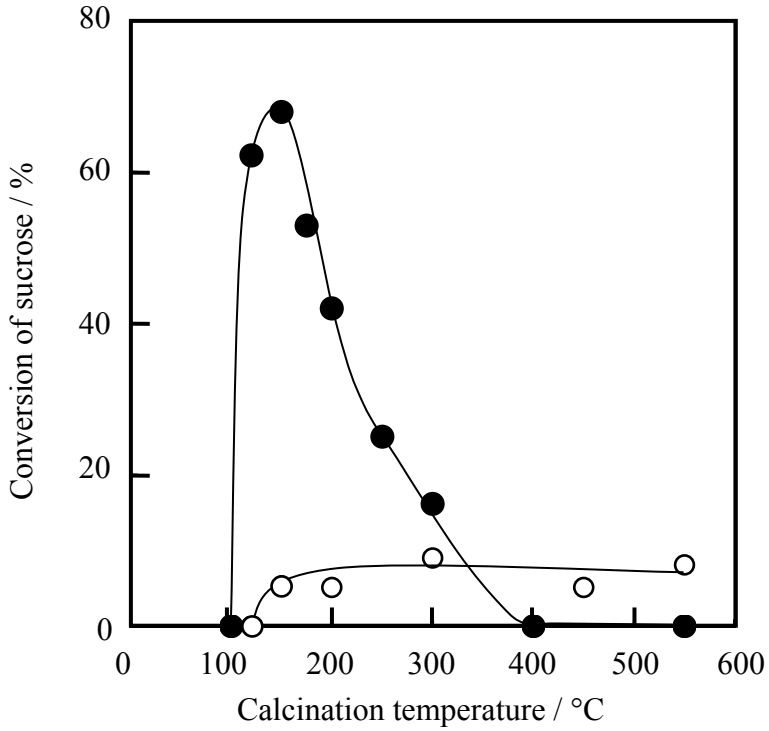
80
60
40
20
0
Conversion of sucrose / %
0
100
200
300
400
500
600
Calcination temperature / °C

Fig. 4

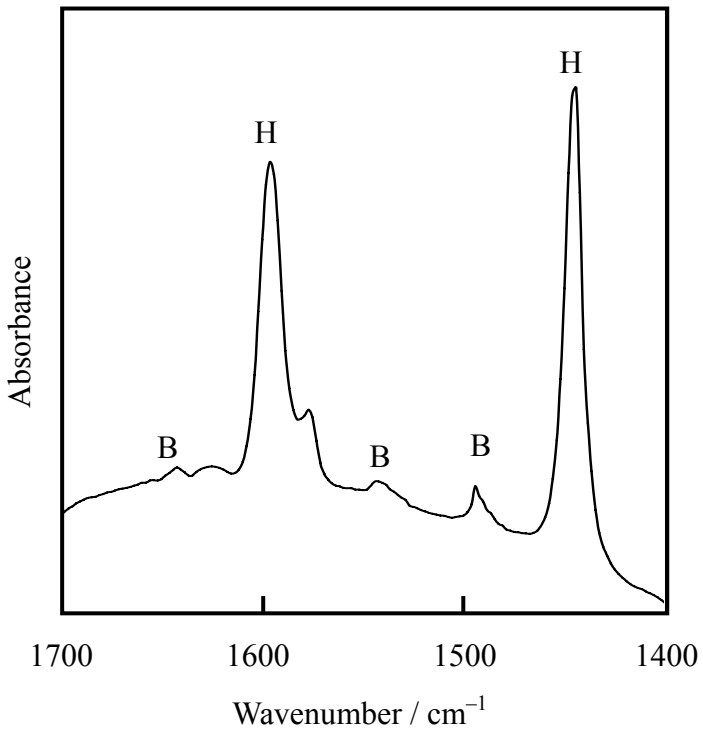

Fig. 5

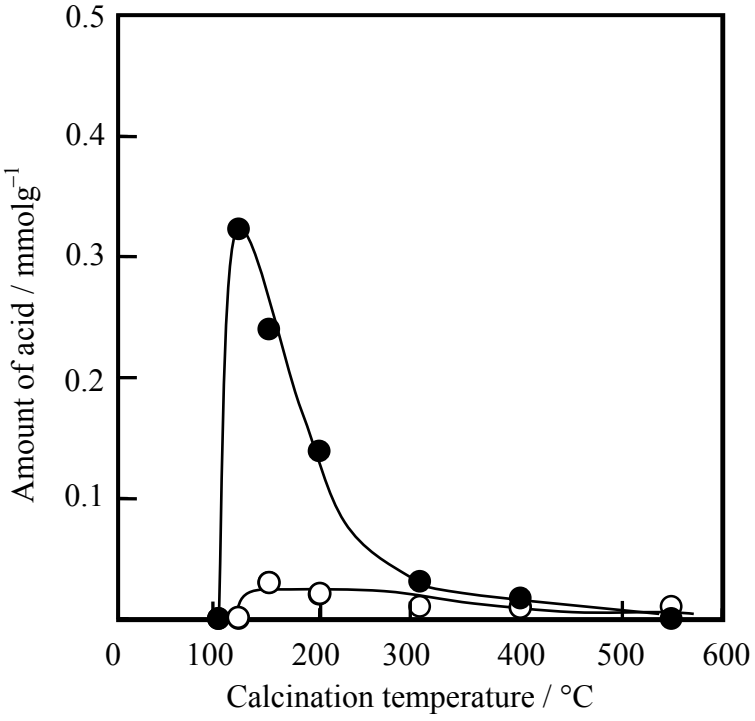
0.5
0.4
0.3
0.2
0.1
Amount of acid / mmolg^{-1}
0
100
200
300
400
500
600
Calcination temperature / °C

Fig. 6

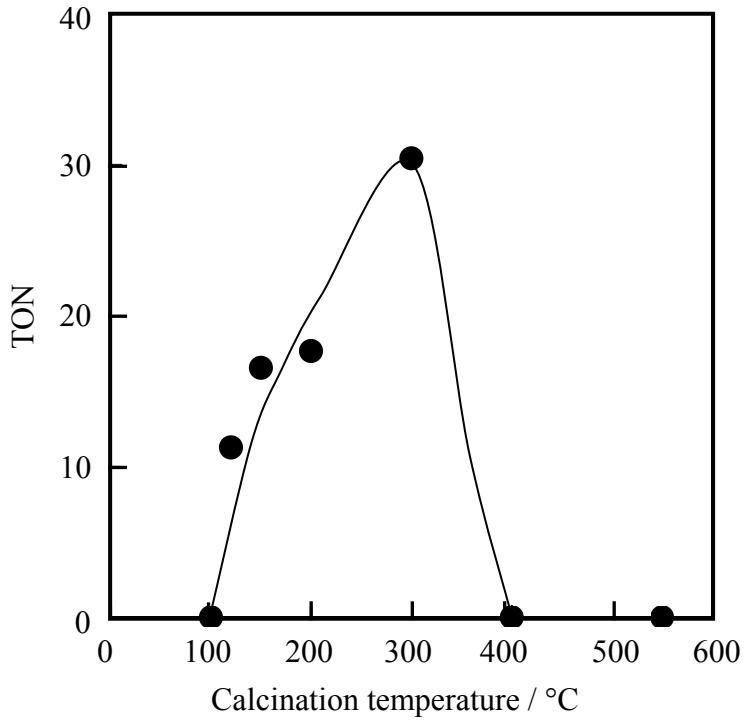
40
30
20
10
0
TON
0
100
200
300
400
500
600
Calcination temperature / °C

Fig. 7

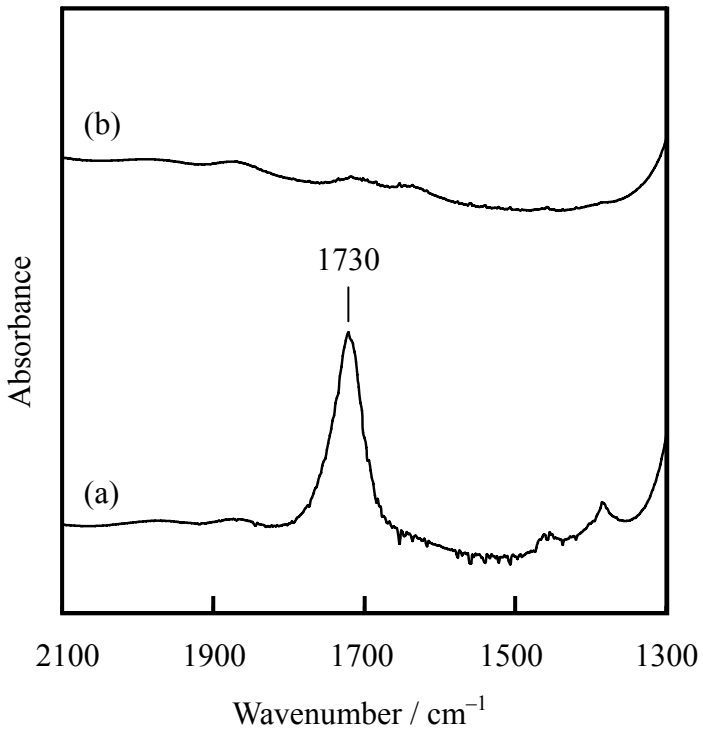

Fig. 8

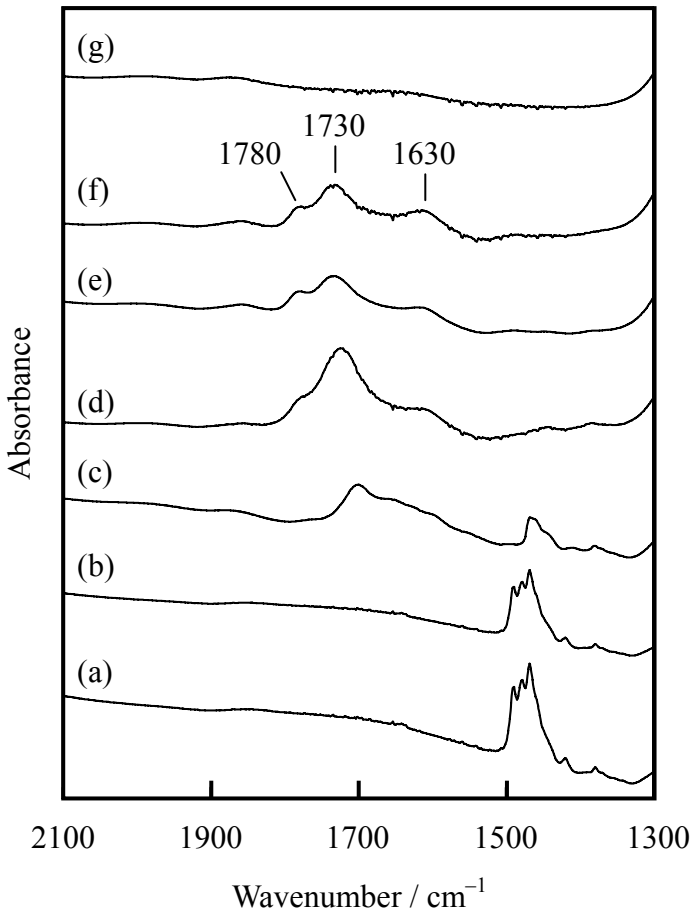
(g)
1730
1780
1630
(f)
(e)
(d)
(c)
(b)
(a)
Absorbance
2100
1900
1700
1500
1300
Wavenumber / cm−1

Fig. 9

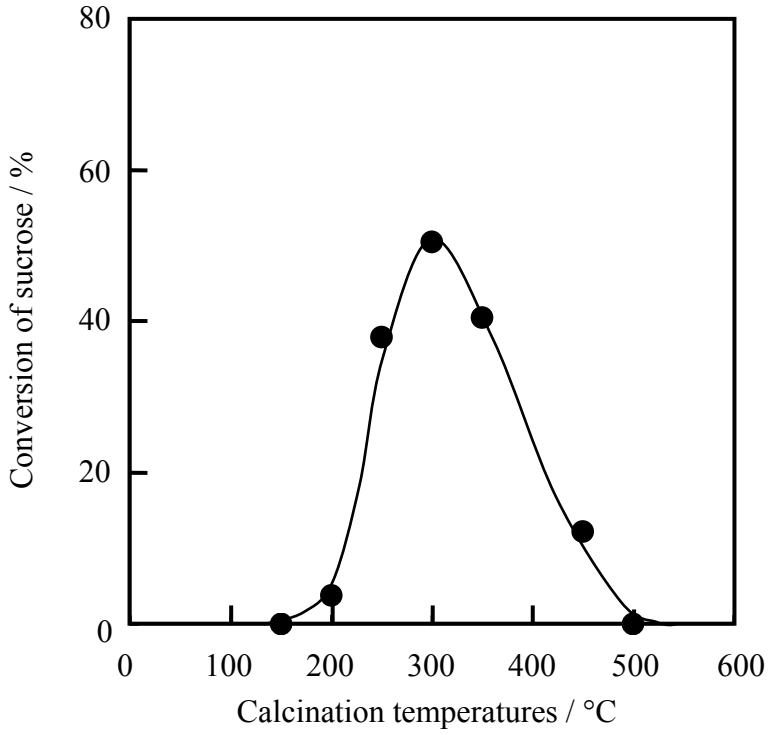
80
60
40
20
0
Conversion of sucrose / %
0
100
200
300
400
500
600
Calcination temperatures / °C

Fig. 10

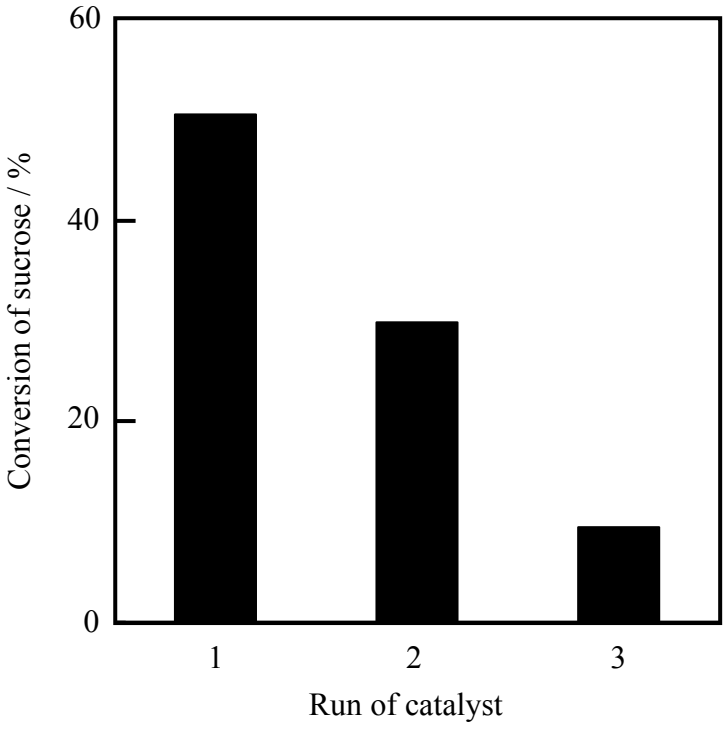

Fig. 11

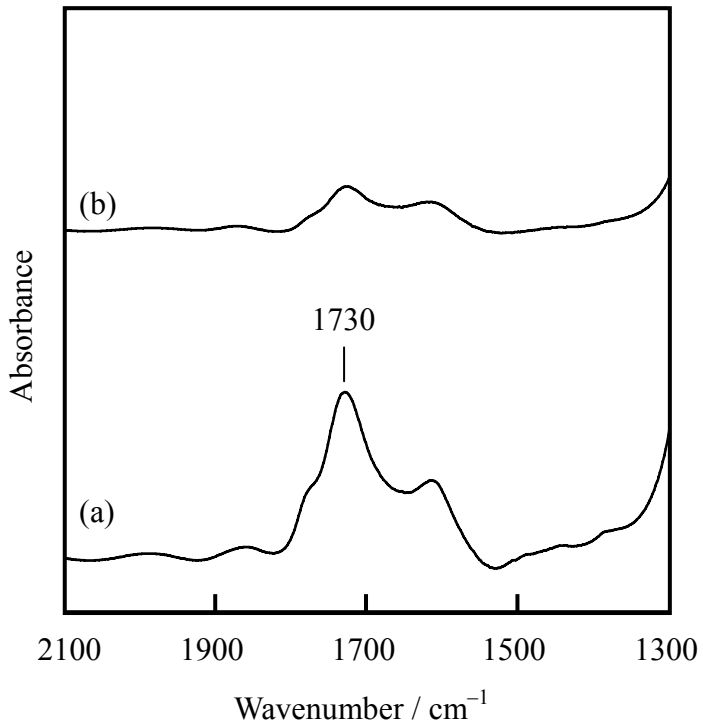

Fig. 12